J Mater Sci (2006) 41:7446–7453
DOI 10.1007/s10853-006-0796-y

Cavitation characteristics of a superplastic 5083 Al alloy during gas blow forming

Horng-yu Wu · Jau-yuean Perng · Shyh-hung Shis · Chui-hung Chiu · Shyong Lee · Jian-yih Wang

Received: 25 March 2005 / Accepted: 5 December 2005 / Published online: 20 September 2006

Abstract Cavitation behavior of a superplastic 5083 Al alloy during gas blow forming has been investigated by deforming the sheet into a die with a rectangular cavity. Cavitation characteristics could be separated into two stages. In stage I, the sheet deformed freely as part of a hemi-cylindrical shape, cavity volume increased exponentially with deformation. The evolution of cavity volume was due to both nucleation and growth of cavities. In the second stage the surface friction would restrict thinning of the sheet, and the cavity volume first increased and then decreased with forming time for all test-forming rates. Decrease in cavity volume in the later stage could be related to the cavity shrinkage rising from sintering effect. A higher strain rate utilizing a higher imposed pressure during blow forming led to a greater average cavity shrinkage rate.

H.-y. Wu (✉) · J.-y. Perng · S.-h. Shis · C.-h. Chiu
Department of Mechanical Engineering, Chung Hua University, 707, Sec2, Wu Fu Rd, Hsinchu 30067, Taiwan, ROC
e-mail: ncuwu@chu.edu.tw

S. Lee
Department of Mechanical Engineering, National Central University, Chungli, Taiwan, ROC

J.-y. Wang
Department of Materials Science and Engineering, National Dong Hwa University, Hualien, Taiwan, ROC

Introduction

Superplastic 5083 (SP) aluminum alloy has attracted interest for the fabrication of automotive sheet parts. Although the SP5083 alloy has a reasonable combination of cost, forming and processing characteristics, a significant problem with this alloy is the internal cavity formation during superplastic deformation. The cavities nucleate at second phase particles or grain boundaries, their subsequent growth and coalescence could cause premature failure during superplastic forming, and the presence of these cavities in the superplastically formed parts would have a deleterious effect on any post-formed applications. Several investigations have been performed to study the characteristics of cavitation during superplastic deformation [1–10]. It is widely accepted that cavity nucleation arises from stress concentrations generated at second phase particles or triple points as a result of grain boundary sliding [1, 11–13]. Cavity nucleation is a very complex problem since cavities can either nucleate or possibly develop from pre-existing cavities. Cavity growth has been studied either experimentally or theoretically. Vacancy diffusion and strain-controlled growth have been proposed as the two main mechanisms for cavity growth [1, 3–5, 14, 15]. The growth rates of these two mechanisms depend on the superplastic conditions, diffusion growth is only predominant at low strain rates and for very small cavities, and cavity growth is essentially strain-controlled during superplastic deformation.

Some fundamental information on the characteristics of cavity development has been obtained. However, most of these studies explored cavitation by use of a tensile test. In order to reduce cavitation levels

it is important to understand the microstructural and deformation parameters that affect the cavitation behavior under multiaxial deformation. The work presented here evaluates the effects of plane strain on cavitation of a SP 5083 Al alloy during superplastic deformation. Gas pressure forming was carried out to deform the sheets into a rectangular die cavity. Focus was placed on the evolution of cavitation during superplastic deformation. The experimental results were quantitatively analyzed and compared with the empirical model.

Experimental

Materials and preparation

Sky Aluminum Company, Japan, provided the SP5083 alloy sheet. The analyzed chemical composition was (wt.%) Al–4.6Mg–0.67Mn–0.1Cr–0.02Cu–0.05Si–<0.05Fe–<0.01Ti. An ingot of the alloy was homogenized at 530 °C for 8 h and hot rolled to a thickness of 6 mm followed by cold rolling to a thickness of 2.0 mm. The sheet was recrystallized at 400 °C for 10 min resulting in an average grain size of 8.6 μm before superplastic deformation.

Grid circles of diameter d_o (2.5 mm) etched on the sheets were used to measure strain levels in each blow-forming test. During forming the etched circles were distorted into ellipses and/or larger circles, and these deformed grid circles were used to measure strain levels in each case [16]. Measurements of the major (d_1), minor (d_2) diameters and thickness (h_3) after deformation were made to determine the principal strains. The effective strain can be expressed as [17]:

$$\bar{\varepsilon} = [2/3(\varepsilon_1^2 + \varepsilon_2^2 + \varepsilon_3^2)]^{1/2} \quad (1)$$

The effect of strain rate on forming was evaluated by the effective strain rate, which can be expressed as

$$\dot{\bar{\varepsilon}} = \frac{\bar{\varepsilon}}{t} = \frac{\sqrt{2}}{\sqrt{3}t}(\varepsilon_1^2 + \varepsilon_2^2 + \varepsilon_3^2)^{1/2} \quad (2)$$

where t is the forming time.

Superplastic deformation procedures

The superplastic sheet was formed into a rectangular die cavity by compressed argon gas. The die had a cavity of 120 mm (length) × 40 mm (width) × 20 mm (depth). The die was made of medium-carbon low alloy steel 4340 with a surface roughness of Ra = 0.84 μm. Incremental step strain rate tensile tests were first conducted covering the range of strain rates from 5×10^{-5} s^{-1} to 1×10^{-2} s^{-1} to determine the superplastic flow characteristics. The variation of strain rate sensitivity index m, over a wide rage of strain rates, with strain was determined by using separate specimens strained to various amounts prior to the step strain rate test. The material constant and m values obtained from the tensile tests were then used for the computer program SUPFORM2 [18] to calculate the pressure profiles for the desired strain rates by using von Mises effective stress and strain concepts. The developed pressure/time cycle for the blow forming maintained a constant strain rate in the unsupported section of the deformed sheet. Test runs were also made to modify the pressure/time cycle predicted by the computer program in order to achieve the desired constant strain rate. The pressure/time cycles used in this work are given in Fig. 1. Gas blow forming was performed at 525 °C and at two different constant strain rates of 1×10^{-3} s^{-1} to 2×10^{-4} s^{-1}. Several interrupted tests were performed to bulge the sheets to various depths for each strain rate, the depth of the central line region, hence the strain, could then be utilized to evaluate the effect of strain on cavitation. In order to obtain the fundamental information on the characteristics of cavity development in SP5083 Al alloy, lubricant and back pressure were not used in this study.

Metallographic inspection

Optical microscopy was used to inspect cavitation of the test piece. The specimens for metallographic examination were mechanically polished and then slightly etched to remove smeared metal covering the cavities. Cavity volume fractions were measured by computer imaging equipment and calculated by using OPTIMAS 5 software [19]. The optical image was first

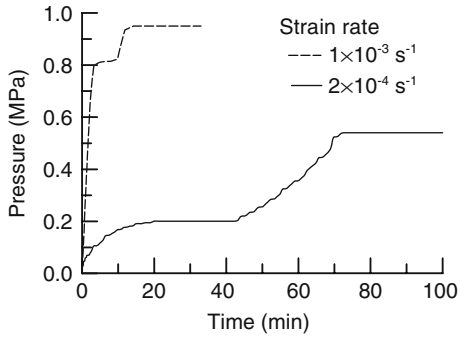

Fig. 1 Pressure–time cycles developed for constant strain rate gas pressure forming

converted into a binary video image. The number of pixels in the cavity (black area) were counted and divided by the total number of pixels in the image to obtained cavity volume fraction.

Results and discussion

Forming into a rectangular die cavity

Since the sheets are bulged to various depths, the configuration of the formed component could be obtained for each test. Figure 2 demonstrates the transverse deformation sequence of the sheet formed at an average strain rate of 1×10^{-3} s^{-1}. The numbers in Fig. 2 represent the forming time for each configuration. The deformation operation for forming into a rectangular die cavity could be considered to separate into two stages. In stage I, the sheet will freely deform as part of hemi-cylindrical shape until it touches the bottom surface of the die. In the second stage of deformation, the sheet is overlaid on the bottom surface and on the sidewall surfaces as the deformation proceeds. After the sheet is deformed into contact with the bottom surface of the die, the surface condition of the die will affect the subsequent deformation of the overlaid region. The thinning of the sheet will be restricted by the surface friction for forming performed without applying lubricant on the die surface; such as the cases carried out in this work.

Figure 3 depicts the thickness distribution of the formed hemi-cylindrical section along the transverse cross section in stage I. No significant thickness variations (except at the die entry) are observed in such a hemi-cylindrical shape forming. For a long rectangular geometry, there is a plane stress state throughout the width of the sheet, and virtually no thinning gradient is seen in stage I. However, on subsequent forming into a die configuration, the die surface can act to restrict deformation in the forming sheet where contact has been made and a thickness gradient will then result in the bulging forming of stage II; as shown in Fig. 4.

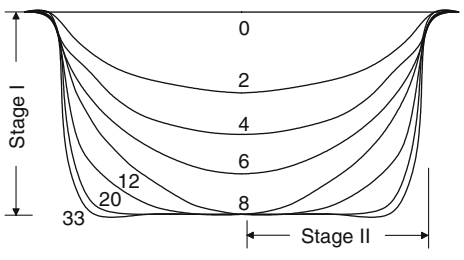

Fig. 2 Experimentally determined transverse deformation sequence with forming time of the sheet formed into a die with a rectangular cavity at a strain rate of 1×10^{-3} s^{-1}; the numbers denoting the forming time (min)

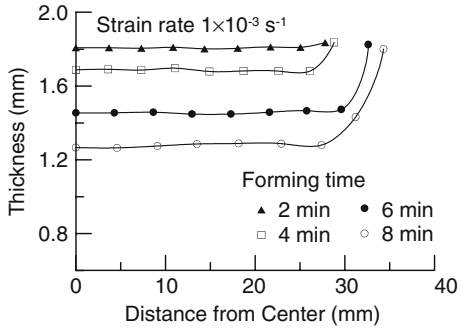

Fig. 3 Thickness distribution of the formed hemi-cylindrical shape along the transverse cross section in stage I of forming at a strain rate of 1×10^{-3} s^{-1}

Cavitation in stage I

Figure 5 illustrates the cavity volume fraction at the central point of the formed parts as a function of effective strain forming at two different strain rates. The decrease in cavitation with strain rate is found in this alloy at the test strain rates of 1×10^{-3} s^{-1} and 2×10^{-4} s^{-1}. This consequence should result from a lower flow stress at a lower strain rate [11]. Since flow stresses influence the stresses built up at grain boundary and thus the tendency for cavity nucleation. A lower flow stress at a lower strain rate means smaller stresses accumulated at grain boundary. Moreover, at a lower strain rate, the stresses generated by the grain boundary sliding would have greater time to become relaxed. Thus, superplastic deformation performed at a lower strain rate could reduce the local stresses at grain boundary irregularities and decrease the cavitation level in SP5083 Al alloy.

The semi-log plots show a linear relationship between cavity volume fraction (plotted logarithmically) and

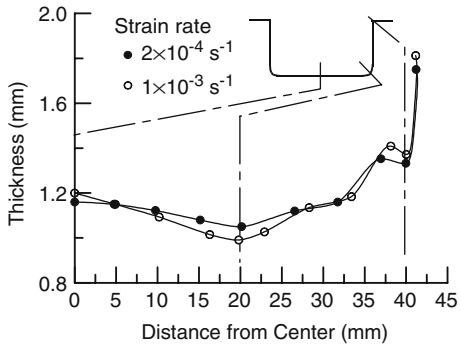

Fig. 4 Thickness distribution of the completely formed rectangular pan along the transverse cross section formed at two different strain rates

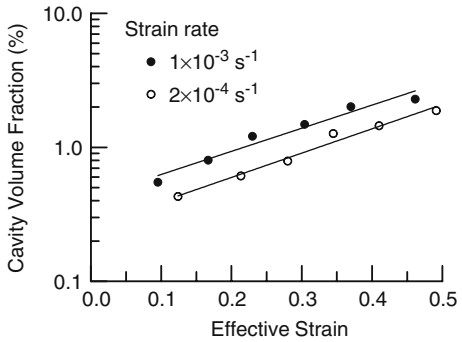

Fig. 5 Cavity volume fraction versus strain showing the effect of strain rate

strain as given in Fig. 5. This result indicates that strain-controlled growth should be the dominant mechanism for the increase of cavity volume fraction. If a strain-controlled growth rate of cavities is assumed [14, 15], the evolution of cavity volume with strain may be expressed as

$$V = V_0 \exp(\eta\varepsilon) \tag{3}$$

where ϵ is strain, η is the cavity growth rate parameter, and V_0 is a fitting constant. Stowell has proposed that the V_0 is the volume fraction of the pre-existing cavities [3]. However, it has been pointed out that V_0 is always a positive value, whether cavities pre-exist or not [20]. Thus V_0 may be related to the tendency of cavity nucleation associated to strain rate.

Following the analysis of Cocks, Ashby and Stowell [3, 4], the cavity growth rate parameter can be shown that

$$\eta = \frac{3}{2}\left(\frac{m+1}{m}\right)\sinh\left[2\left(\frac{2-m}{2+m}\right)\frac{k_s}{3}\right] \tag{4}$$

where m is the strain-rate sensitivity index, k_s is a geometric factor whose value depends on the test geometry (uniaxial, equi-biaxial or plane strain) and the extent of grain boundary sliding [21]. For most superplastic alloys about 50% of the accumulated strain is believed to be due to grain boundary sliding, thus the value of $k_s = 2.02$ could be adopted for plane strain deformation [14]. In Table 1, the values of η with strain rate (m value) predicated by Eq. 4 are given and compared with those determined from the experimental data. It is found that V_0 is indeed related to strain rate. V_0 decreases with decreasing strain rate and is sensitive to strain rate. The calculated values of η are smaller than those determined experimentally. The difference is most likely to be caused by a combination of two factors. Firstly, the m value to the material changes with strain. Secondly, continuous cavity nucleation and cavity coalescence during deformation will cause an increase in the cavity growth rate.

The variations of m with strain rate at several strains and with strain determined by incremental step strain rate tensile tests are illustrated in Fig. 6. The variation of m with strain during deformation at a given strain rate is dependent on the superplastic behavior of the material. If the deformation strain rate is greater and near the strain rate with maximum m value, the m value decreases with increasing strain. If the deformation strain rate is less than the strain rate of the maximum m value, the m value may first increase with increasing strain then decrease [14]. The m value of the superplastic 5083 alloy decreases progressively with strain for strain rates used in this study; as shown in Fig. 6. As the m value decreases with increasing strain during deformation, the cavity growth rate parameter, η, should increase. Therefore, greater values of η are observed.

Equation 4 is basically deduced from the model proposed by Cocks and Ashby [4]. Cavity nucleation and cavity coalescence during deformation were not taken into account in this model. It has been found that the cavity volume fraction increases with strain not only due to the increasing cavity size but also due to the increasing cavity number [22–24]. A plot of total number density of cavities (number mm^{-2}) as a function of effective strain is given in Fig. 7. It shows that the total number of cavities increases with increasing strain. The increase of total number density of cavities due to cavity nucleation can be observed from the actual distribution of cavity sizes and their variation with forming time. Figure 8 shows the number density of cavities as a function of cavity size forming at two different strain rates. The density for all cavity sizes appears to increase with forming, especially for the smallest cavity size (~2 μm). These results reveal that new cavities continue to nucleate during deformation as cavity growth occurs. The development of a high-radius tail with increasing forming time indicates cavity coalescence does take place; as shown in Fig. 8. The

Table 1 Comparison of the calculated and experimentally determined cavitation parameters

Strain rate (s^{-1})	m value	η (Calculated)	η (Experiment)	V_0 (Experiment)
1×10^{-3}	0.54	3.65	3.97	0.422
2×10^{-4}	0.51	3.94	4.18	0.259

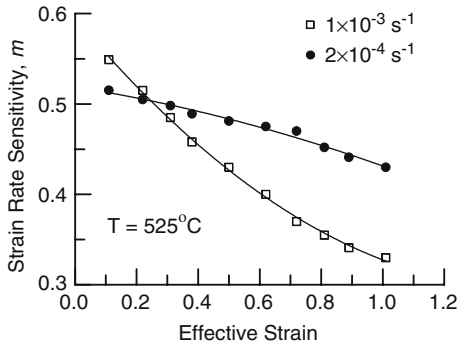

Fig. 6 Variation of strain rate sensitivity with strain during deformation at two different strain rates

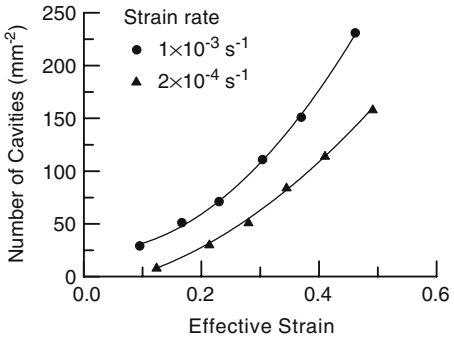

Fig. 7 Total number of cavities per unit area versus strain showing the effect of strain rate

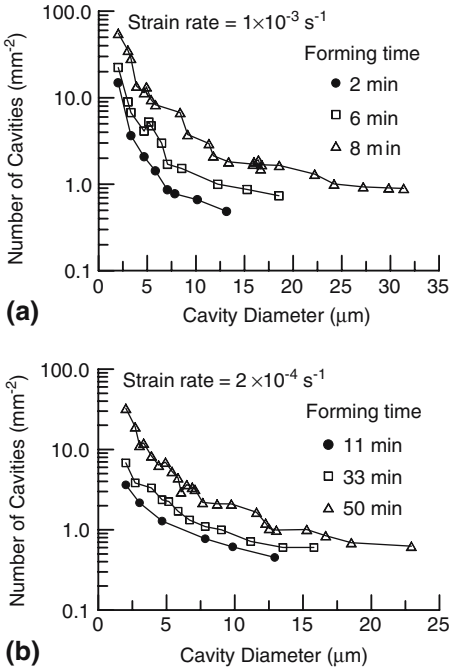

Fig. 8 Number of cavities per unit area versus cavity diameter at various forming time formed at two different strain rates (**a**) 1×10^{-3} s^{-1}, (**b**) 2×10^{-4} s^{-1}

effect of cavity nucleation and coalescence is to increasingly raise the cavity volume towards the longer forming time and hence give higher values of η than predicted by Eq. 4. Figure 9 shows the micrograph of cavitation in the formed pan at the central region deformed to a strain of 0.5 for forming at a strain rate of 1×10^{-3} s^{-1}. It could be noticed that some void coalescence does occur during deformation.

Figure 7 also indicates that the higher strain rate produces quite large number of cavities in the early stage of deformation. In a fine-grained superplastic material, grain boundary sliding is the dominant mechanism of deformation during superplastic forming. Grain boundary sliding is believed to cause the development of stress concentration at sites where sliding is impeded. If the stress concentrations are not attenuated rapidly by processes like local diffusion flow or plastic deformation, to meet the requirements imposed by the deformation rate, cavity nucleation occurs at these sites. The number of nucleation sites would be high due to the high flow stress at the higher strain rate resulting in large number of cavities.

Cavitation in stage II

Figure 10a depicts the evolution of cavity volume fraction and the thickness at the central region of the deformed sheet with forming time for the deformation at a strain rate of 1×10^{-3} s^{-1}. For forming at a strain rate of 1×10^{-3} s^{-1}, the center of the sheet touches the bottom surface at around 8 min, and it takes about 33 min for completely forming a rectangular pan. Hence, the time span from 8 to 33 min accounts for the deformation of stage II. In this stage, the cavity volume fraction of the central region keeps on increasing in the early stage, it reaches a maximum value at a forming time around 16 min, then it decreases till the end of forming, as shown in Fig. 10a. The variation of cavity

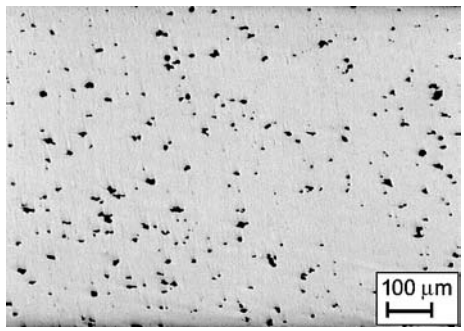

Fig. 9 Optical micrograph showing cavitation at the central region of the pan deformed to an effective strain of 0.5 at a strain rate of 1×10^{-3} s^{-1}

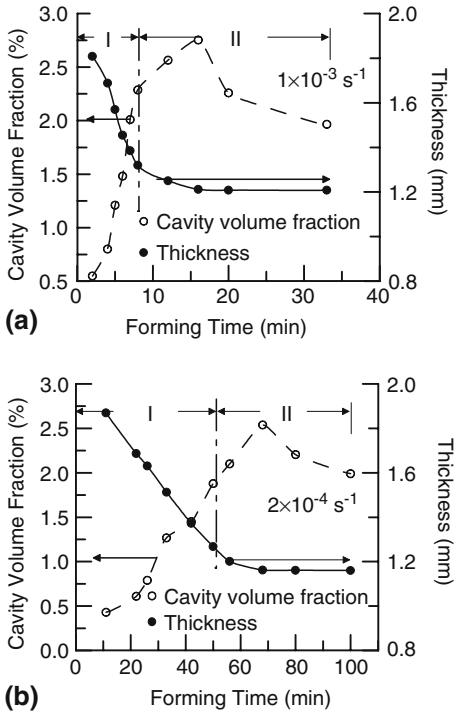

Fig. 10 Evolution of cavity volume fraction and thickness at the central region of the formed part versus forming time at two different strain rates. (**a**) 1×10^{-3} s^{-1}, (**b**) 2×10^{-4} s^{-1}

volume fraction with time in stage II could be associated to the thinning behavior of the sheet. The thickness of the central point decreases with increasing forming time, it reaches a thickness about 1.21 mm at a forming time around 16 min and then remains almost as a constant. Changes of cavity volume fraction in stage II are associated to the variations of the thickness at the central point of the deformed sheet. The cavity volume fraction increases with decrease in thickness in the early stage of stage II, it begins to decrease as significant thinning of the deformed sheet brings to an end. It is believed that cavity closure occurs giving rise to the decrease in cavity volume fraction in the later stage during superplastic forming while the sheet has been overlaid on the die surface.

Similar results are also observed for forming at a lower strain rate; as shown in Fig. 10b. The deformed sheet comes into contact with the bottom surface of the die at a forming time around 50 min for forming at a strain rate of 2×10^{-4} s^{-1}. The maximum cavity volume fraction occurs at the forming time about 68 min, this is also the time that significant thinning of the sheet stops.

Decrease in cavity volume fraction in the later stage for forming a superplastic sheet into a die with rectangular geometry could be related to the cavity shrinkage as a result of sintering effect. After the significant thinning of the deformed sheet is prevented by the restriction of the surface friction, decrease in cavity volume in the region at which significant thinning does not occur could be described as the sintering of cavities at elevated temperature under pressure. A plot of the number density of cavities as a function of cavity size forming at two different strain rates is given in Fig. 11 to illustrate the effect of the cavity shrinkage in the later stage of forming. The decrease of the high-radius tail with increasing forming time indicates that cavity shrinkage does take place. The density for the smallest cavity size (~2 μm) also appears to increase with forming time. Since the thickness at the central region almost remains as a constant in the later stage of forming, no significant deformation is observed, increase in the density of the smallest cavity should not be resulted from cavity nucleation. Figure 12 illustrates the variation of mean cavity diameter at the central region of the formed pans with forming time. The decrease in mean cavity diameter in the later stage of forming also points out that cavity shrinkage does occur in this time span. Micrographs in the later stage of forming showing the progression of cavitation of the pans from the central locations formed at a strain rate of 1×10^{-3} s^{-1} are given in Fig. 13. It is also seen in the micrographs that the number of the

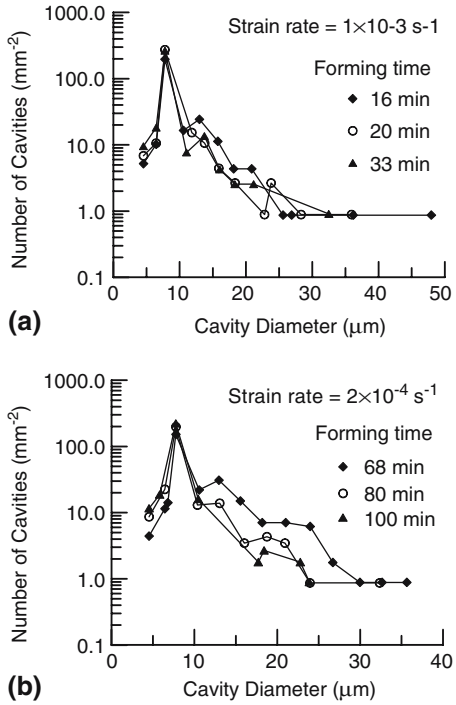

Fig. 11 Number of cavities per unit area versus cavity diameter at various forming time formed at two different strain rates. (**a**) 1×10^{-3} s^{-1}, (**b**) 2×10^{-4} s^{-1}

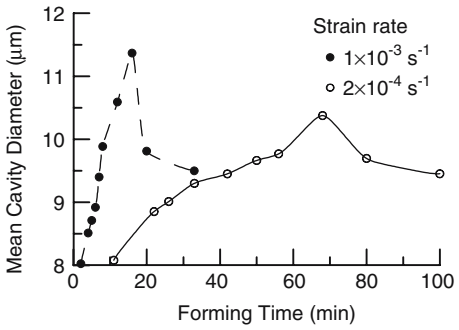

Fig. 12 Variation of mean cavity diameter at the central region of the formed parts versus forming time at two different strain rates

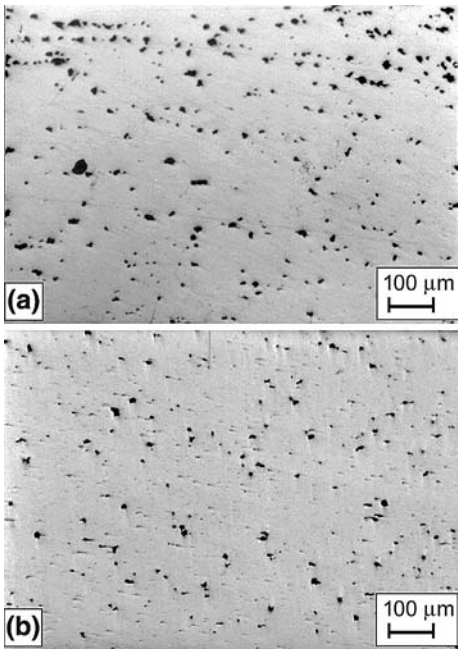

Fig. 13 Micrographs showing the progression of cavitation at the central region of formed pans at a strain rate of 1×10^{-3} s^{-1}. (**a**) Forming time = 16 min, (**b**) Forming time = 33 min

small-sized cavity decreases and the size of the large cavity decreases, as forming proceeds from 16 to 20 min.

For plasticity controlled cavity shrinkage mechanism, the imposed external pressure has a significant effect on the cavity shrinkage rate [25]. In the present work, the imposed forming pressures in the later stage are 0.95 and 0.54 MPa for the strain rates of 1×10^{-3} s^{-1} and 2×10^{-4} s^{-1}, respectively. In the later stage of stage II, no significant thinning occurs in the overlaid regions; hence strain rate is not responsible for the variation of the cavitation levels in these regions. The imposed pressure is then the major factor to cause the changes of cavity volume fraction. A greater imposed pressure accelerates cavity closure resulting in a higher average cavity shrinkage rate for forming at a strain rate of 1×10^{-3} s^{-1}.

Conclusions

An analysis of cavitation characteristics of a SP5083 Al alloy through usage of blow forming was undertaken in the present study. Cavitation characteristics due to plane strain deformation were analyzed and compared with the empirical model. The following conclusions were determined on the basis of this work:

1. The formation of a rectangular pan during superplastic forming could be divided into two stages. In the first stage, the sheet deformed freely into a hemi-cylindrical shape until its central region contacted the bottom surface of the die. The second stage started when the sheet just touched the bottom surface of the die. The central region of the deformed sheet was overlaid on the bottom surface of the die as the deformation proceeded, the surface friction of the die would influence the deformation of the overlaid region of the deformed sheet in stage II. Therefore, cavitation behavior during deformation should be examined separately in theses two stages.
2. In stage I, the relationship between the cavity volume fraction and strain was consistent with cavity growth dominated by plasticity-controlled mechanism. The values of cavity growth rate parameter, η, determined experimentally in this work were greater than those calculated by empirical model. Changes of m value with strains, continuous cavity nucleation and cavity coalescence during deformation should be the possible factors to cause the difference.
3. In the second stage of deformation, variation of cavity volume fraction was related to the thinning behavior of the deformed sheet. The cavity volume fraction increased with decreasing thickness, and it turned to decrease while the thickness of the sheet remained as a constant. Decrease in cavity volume was believed to be the result of cavity sintering effect. A higher imposed pressure for forming at a higher strain rate resulted in a greater average cavity closure rate.

Acknowledgements This work was conducted through grant from National Science Council under the contract NSC 91-2212-E-216-009.

References

1. Raj R, Ashby MF (1975) Acta Metall 23:653
2. Wu HY (2000) J Mater Processing Tech 101:76
3. Stowell MJ, Liversy DW, Ridley N (1984) Acta Metall 32:35
4. Cocks ACF, Ashby MF (1982) Metal Sci 16:465
5. M. Suery (1985) In: Baudelet B, Suery M (eds) Proceedings Of Superplasticity, Grenoble, France, September 1985. Centre National De La Recherche Scientifique, Paris, p 9.1
6. Zelin MG, Yang HS, Valiev RZ, Mukherjee AK (1993) Metall Trans A 24A:417
7. Wu HY (2000) Mater Sci Eng A A291:1–8
8. Verma R, Friedman PA, Ghosh AK, Kim S, Kim C (1996) Metall Trans A 27A:1889
9. Ghosh AK, Bae DH (1997) In: Chokshi AH (ed) Proceedings of Superplasticity in Advanced Materials ICSAM-97, Bangalore, India, January 1997. Trans Tech Publications, Switzerland, 1997, p 89
10. Wu HY (2000) Mater Manuf Processes 15:231
11. Stowell MJ (1983) Metal Sci 17:1
12. Geckinli AE (1983) Metal Sci 17:12
13. Gifkins RC (1976) Metall Trans A 17A:1225
14. Pilling J, Ridley R (1986) Acta Metall 34:669
15. Pilling J (1985) Mater Sci Tech 1:461
16. Mahoney MW, Hamilton CH, Ghosh AK (1983) Metall Trans A 14A:1593
17. Dieter GE (1988) In: Mechanical metallurgy. Mcgraw-Hill Book Company, London, p 87
18. CEMEF (1989) SUPFORM2 User's Guide, Version 1.0. Fcole Des Mines De Paris
19. Optimas Corporation (1995) Optimas 5 Software, 6th edn. P.O. Box 24467, Seattle, Washington 98124-0467
20. Chokshi AH, Mukherjee AK (1989) Acta Metall 37:3007
21. Pilling J, Ridley N (1989) In: Superplasticity in crystalline solids. The Institute of Metals, London, p 102
22. Bae DH, Ghosh AK (2002) Acta Mater 50:993
23. Bae DH, Ghosh AK (2002) Acta Mater 50:1011
24. Gouthama, Padmanabhan KA (2003) Scripta Mater 49:761
25. Varloteaux A, Blandin JJ, Suery M (1989) Mater Sci Tech 5:1109